# PERFORMANCE STUDY OF A CHOPPER-CONTROLLED INDUCTION MOTOR USING TENSOR TECHNIQUE

**M.Y. Abdelfattah and A.R. Abdelaziz**
Electrical Engineering Department
Faculty of Engineering, Alexandria University
Alexandria, Egypt.

ABSTRACT

In this paper, the speed of an induction motor is controlled using a chopper circuit on the rotor side. Analysis of transient, including switching power supply and changing in duty cycle of chopper, and steady-state performance of the chopper-controlled induction motor are predicted. Analysis and simulation are based on tensor technique. Experimental results are obtained to verify predicted behaviour based on this digital simulation.

## NOMENCLATURE

| | |
|---|---|
| A,B,C | Suffices indicating stator variables as in $v_A$ |
| a,b,c | Suffices indicating rotor variables as in $v_a$ |
| s | Suffix indicating stator quantity as in $L_s$ |
| r | Suffix indicating rotor quantity as in $L_r$ |
| q,d | Suffices indicating q and d axes respectively |
| $i_{qs}$,$i_{ds}$ | Two-phase q,d axes stator currents |
| $i_{qr}$,$i_{dr}$ | Two-phase q,d axes rotor currents |
| $v_{ds}$,$v_{ds}$ | Two-phase q,d axes stator voltages |
| $v_{qr}$,$v_{dr}$ | Two-phase q,d axes rotor voltages |
| $R_s$ | Resistance of one stator phase |
| $R_r$ | Resistance of one rotor phase |
| $L_s$ | Apparent three phase stator inductance per phase |
| $L_r$ | Apparent three phase rotor inductance per phase |
| M | Apparent three phase mutual inductance per phase |
| $\omega_r$ | Rotational frequency of the machine rotor |
| $\theta$ | Angle between stator phase A and rotor phase a |
| J | Rotor moment of inertia |
| $T_E$ | Electromagnetic torque developed |
| $T_L$ | Load torque |
| $T_D$ | Damping torque |
| $R_F$,$L_F$ | Filter resistance and inductance respectively |
| $R_{add}$ | Added resistance to rotor side |
| $T_{CH}$ | The chopper chopping period |
| $T_{ON}$ | The chopper on period |
| $\lambda$ | The chopper duty cycle ($\lambda = T_{ON}/T_{CH}$) |
| $i_{link}$ | Instantaneous filter current |
| $v_{dc}$ | Instantaneous dc rectifier output voltage |
| $v_{ad}$ | Instantaneous line-to-line voltage between points a and b |
| p | Operator d/dt |
| $\alpha$,$\beta$ | Orthogonal rotating two-phase axes |

## INTRODUCTION

Connection of resistors to the slip-rings of an induction motor can improve starting conditions and give speed adjustment. Different attempts have been made to use SCR's in different configurations in the rotor circuit to have continuous and contactless effective rotor impedance control [1-4]. In references [2]-[4] the effective rotor resistance is controlled by varying the duty cycle of the copper. The technique is relatively economical for low and medium power applications and is easy to use for closed control systems. In these references, analysis and simulation are based on the dc model. The dc model introduced is based on the previous assumptions of:

1. Only two diodes are conducting. With this assumption the overlap angle (commutation angle) will be neglected.
2. The effect or ripple in bridge output current is negligible. This will be the case if the filter has a high inductance to keep the current nearly smooth.
3. The chopper-controlled external resistance will be replaced by a fictitious average resistance. With this assumption, for a given duty cycle, the rectified current is proportional to motor slip.

Based on the previous three assumptions the rectified voltage is constant and the torque developed by the motor under steady-state becomes a linear function of the rectified current. Therefore, the dc model will not be able to predict the various modes of motor operation under both transient and steady-state performance for normal

and abnormal system operating conditions.

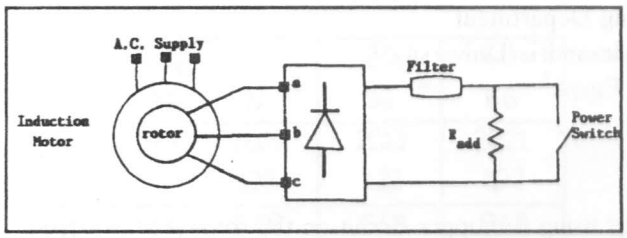


Figure 1. Chopper-Controlled Induction Motor.

Figure (1) shows the system suggested for study. In this system, the filter is used to minimize the harmonic contents in the ac component of the rectified rotor current. The system performance during transient and steady-state operations is studied using tensor technique.

## INDUCTION MACHINE EQUIVALENT CIRCUIT REFERRED TO ROTOR USING d-q MODEL

The study of the transient performance of three phase induction motor and their behaviour on non-sinusoidal supplies is much easier with transformation of the machine variables to a reference frame in which there is a stationary reference frame. They are called the direct, and the quadrature, axes [5]. Since the choice of time-zero is arbitrary, it is most convenient to choose time-zero at the instant when q,A and a axes are all coincident as shown in Figure (2). Choosing an instant when the $\alpha$-axis of the rotating two phase axes ($\alpha$,$\beta$) makes an angle $\theta$ with the stationary q-axis, and assuming no zero-sequence components, one form of transformation of rotor quantities between rotating three-phase (a,b,c) and stationary two-phase (d,q) is:

$$\begin{bmatrix} v_a \\ v_b \\ v_c \end{bmatrix} = \begin{bmatrix} \cos\theta & -\sin\theta \\ \cos(\theta+120^\circ) & -\sin(\theta+120^\circ) \\ \cos(\theta-120^\circ) & -\sin(\theta-120^\circ) \end{bmatrix} \begin{bmatrix} v_{qr} \\ v_{dr} \end{bmatrix} \quad (1)$$

and

$$\begin{bmatrix} i_a \\ i_b \\ i_c \end{bmatrix} = \begin{bmatrix} \cos\theta & -\sin\theta \\ \cos(\theta+120^\circ) & -\sin(\theta+120^\circ) \\ \cos(\theta-120^\circ) & -\sin(\theta-120^\circ) \end{bmatrix} \begin{bmatrix} i_{qr} \\ i_{dr} \end{bmatrix} \quad (2)$$

Also, we can define the (d,q) stator voltage as:

$$\begin{bmatrix} v_{qs} \\ v_{ds} \end{bmatrix} = \begin{bmatrix} 1 & 0 & 0 \\ 0 & -\frac{1}{\sqrt{3}} & \frac{1}{\sqrt{3}} \end{bmatrix} \begin{bmatrix} v_A \\ v_B \\ v_C \end{bmatrix} \quad (3)$$

The above transformations do not give invariance of power, but this is not important in this case since variables are ultimately expressed in the three-phase reference frame.

Using per-unit quantities, the differential equations describing the behaviour of the machine when referred to the stationary frame can be written in the form:

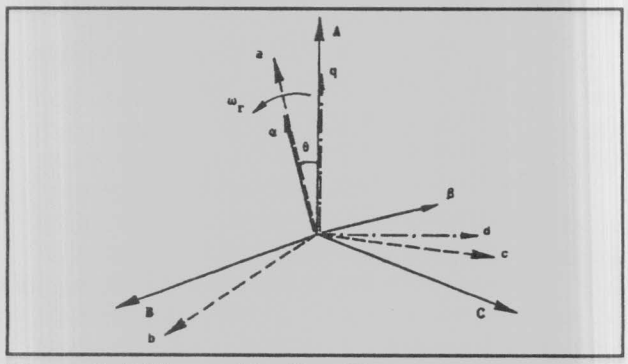


Figure 2. Different Machine Phase Axes.

$$\begin{bmatrix} v_{qs} \\ v_{ds} \\ v_{qr} \\ v_{dr} \end{bmatrix} = \begin{bmatrix} R_s & 0 & 0 & 0 \\ 0 & R_s & 0 & 0 \\ 0 & -\omega_r M & R_r & -\omega_r L_r \\ \omega_r M & 0 & \omega_r L_r & R_r \end{bmatrix} \begin{bmatrix} i_{qs} \\ i_{ds} \\ i_{qr} \\ i_{dr} \end{bmatrix} + \begin{bmatrix} L_s & 0 & M & 0 \\ 0 & L_s & 0 & M \\ M & 0 & L_r & 0 \\ 0 & M & 0 & L_r \end{bmatrix} p \begin{bmatrix} i_{qs} \\ i_{ds} \\ i_{qr} \\ i_{dr} \end{bmatrix} \quad (4)$$

Equation (4) can be rearranged as:

$$\begin{aligned} pi_{qs} &= [L_r v_{qs} - M v_{qr} - \omega_r M^2 i_{ds} - \omega_r M L_r i_{dr} \\ &\quad - L_r R_s i_{qs} + M R_r i_{qr}]/(L_r L_s - M^2) \\ pi_{ds} &= [L_r v_{ds} - M v_{dr} - \omega_r M^2 i_{qs} - \omega_r M L_r i_{qr} \\ &\quad - L_r R_s i_{ds} + M R_r i_{dr}]/(L_r L_s - M^2) \\ pi_{qr} &= [-M v_{qs} + L_s v_{qr} + \omega_r L_s M i_{ds} + \omega_r L_s L_r i_{dr} \\ &\quad + M R_s i_{qs} - L_s R_r i_{qr}]/(L_r L_s - M^2) \\ pi_{dr} &= [-M v_{ds} + L_s v_{dr} - \omega_r M L_s i_{qs} - \omega r L_s L_r i_{qr} \\ &\quad + M R_s i_{ds} - L_s R_r i_{dr}]/(L_r L_s - M^2) \end{aligned} \quad (5)$$

In per-unit quantities the electromagnetic torque $T_E$ becomes:

$$T_E = M[i_{dr} i_{qs} - i_{qr} i_{ds}] \quad (6)$$

Also, from balance between input and output:

$$T_E = Jp\omega_r + T_D + T_L \quad (7)$$

Equation (7) can be rearranged as:

$$p\omega_r = [T_E - T_D - T_L]/J \quad (8)$$

$$p\theta = \omega_r \quad (9)$$

Substituting equations (4) and (5) into equation (1) and then substituting for $i_{qr}$ and $i_{dr}$ using equation (2) we get:

$$\begin{aligned} v_a &= [R_r + pL_{eq}] i_a + [\omega_r (L_{eq} - L_r) i_{dr} - \omega_r M i_{ds} - (MR_s/L_s) i_{qs} \\ &\quad + (M/L_s) v_{qs}] \cos\theta - [\omega_r (L_r - L_{eq}) i_{qr} + \omega_r M i_{qs} \\ &\quad - (MR_s/L_s) i_{ds} + (M/L_s) v_{ds}] \sin\theta \end{aligned} \quad (10)$$

$$\begin{aligned} v_b &= [R_r + pL_{eq}] i_b + [\omega_r (L_{eq} - L_r) i_{dr} - \omega_r M i_{ds} - (MR_s/L_s) i_{qs} \\ &\quad + (M/L_s) v_{qs}] \cos(\theta + 120^\circ) - [\omega_r (L_r - L_{eq}) i_{qr} + \omega_r M i_{qs} \\ &\quad - (MR_s/L_s) i_{ds} + (M/L_s) v_{ds}] \sin(\theta + 120^\circ) \end{aligned} \quad (11)$$

$$\begin{aligned} v_c &= [R_r + pL_{eq}] i_c + [\omega_r (L_{eq} - L_r) i_{dr} - \omega_r M i_{ds} - (MR_s/L_s) i_{qs} \\ &\quad + (M/L_s) v_{qs}] \cos(\theta - 120^\circ) - [\omega_r (L_r - L_{eq}) i_{qr} + \omega_r M i_{qs} \\ &\quad - (MR_s/L_s) i_{ds} + (M/L_s) v_{ds}] \sin(\theta - 120^\circ) \end{aligned} \quad (12)$$

where;

$$L_{eq} = (L_r L_s - M^2)/L_s \quad (13)$$

Equations (10)-(12) can be represented by the equivalent circuit shown in Figure (3), where;

$$\begin{aligned} v_G &= [\omega_r (L_{eq} - L_r) i_{dr} - \omega_r M i_{ds} - (MR_s/L_s) i_{qs} \\ &\quad + (M/L_s) v_{qs}] \cos\theta - [\omega_r (L_r - L_{eq}) i_{qr} + \omega_r M i_{qs} \\ &\quad - (MR_s/L_s) i_{ds} + (M/L_s) v_{ds}] \sin\theta \end{aligned} \quad (14)$$

$$\begin{aligned} v_H &= [\omega_r (L_{eq} - L_r) i_{dr} - \omega_r M i_{ds} - (MR_s/L_s) i_{qs} \\ &\quad + (M/L_s) v_{qs}] \cos(\theta + 120^\circ) - [\omega_r (L_r - L_{eq}) i_{qr} + \omega_r M i_{qs} \\ &\quad - (MR_s/L_s) i_{ds} + (M/L_s) v_{ds}] \sin(\theta + 120^\circ) \end{aligned} \quad (15)$$

$$\begin{aligned} v_K &= [\omega_r (L_{eq} - L_r) i_{dr} - \omega_r M i_{ds} - (MR_s/L_s) i_{qs} \\ &\quad + (M/L_s) v_{qs}] \cos(\theta + 120^\circ) - [\omega_r (L_r - L_{eq}) i_{qr} + \omega_r M i_{qs} \\ &\quad - (MR_s/L_s) i_{ds} + (M/L_s) v_{ds}] \sin(\theta - 120^\circ) \end{aligned} \quad (16)$$

$$Z_{eq} = [R_r + pL_{eq}] \quad (17)$$

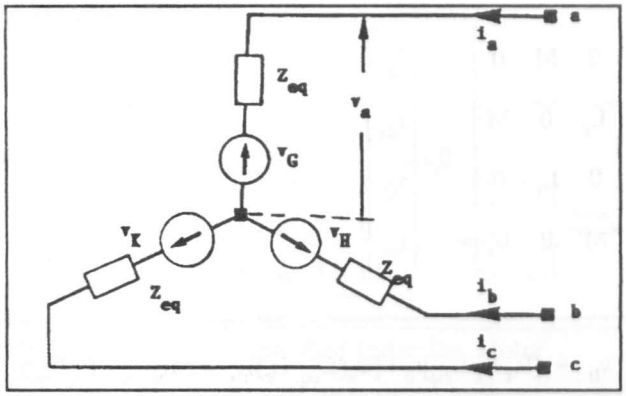


Figure 3. Equivalent Circuit for an Induction Machine Referred to Rotor Side.

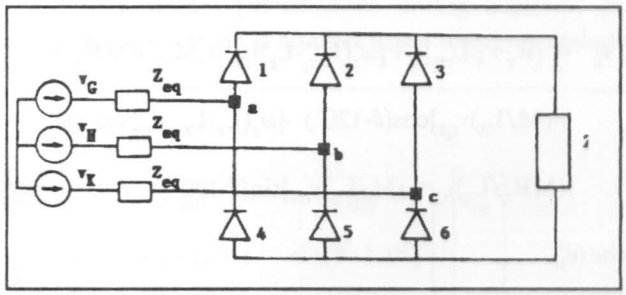


Figure 4. Modified Circuit for Chopper-Controlled Induction Motor.

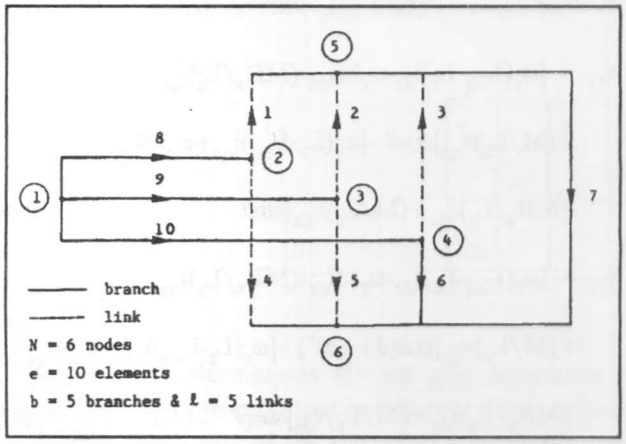


Figure 5. Tree and Cotree for the Circuit Shown in Figure (4).

## ANALYSIS

Figure (4) shows a modified circuit for the chopper-controlled induction motor. When the power switch is in the ON mode, the equivalent resistance in the rotor circuit is $R_F$. When the switch is in the OFF mode, the equivalent resistance is $(R_F+R_{add})$. During ON/OFF operation the equivalent impedance $Z_L$ varies from $[R_F+pL_F]$ to $[(R_F+R_{add})+pL_F]$ respectively. Figure (5) gives the oriented connected graph for the circuit shown in Figure (4). Choosing branches 1,2,3,4 and 5 as links, we obtain five basic loops. Each basic loop contains only one link as shown in Figure (6). The performance equation of the network in the loop reference frame [6] can be written in the form:

$$E_{loop} = Z_{loop} I_{loop} \tag{18}$$

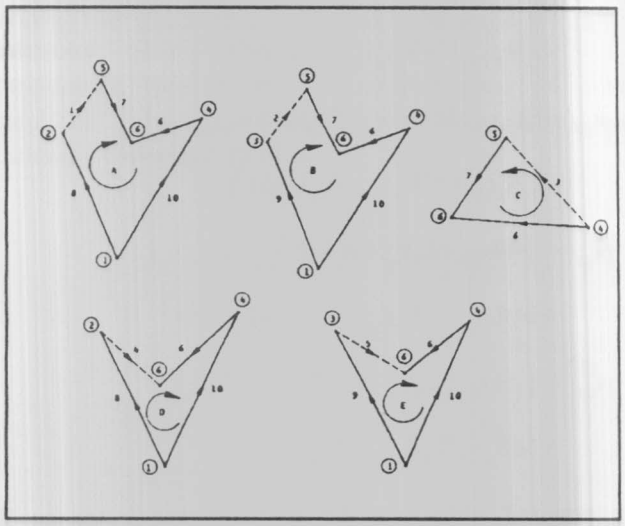

Figure 6. Basic Loops for the Tree and Cotree Shown in Figure (5).

From the previous choice of the basic loops shown in Figure (6), we conclude that:

$$E_{loop} = \begin{matrix} A \\ B \\ C \\ D \\ E \end{matrix} \begin{bmatrix} v_G - v_K \\ v_H - v_K \\ 0 \\ v_G - v_K \\ v_H - v_K \end{bmatrix} \tag{19}$$

$$I_{loop} = \begin{matrix} A \\ B \\ C \\ D \\ E \end{matrix} \begin{bmatrix} I_A \\ I_B \\ I_D \\ I_D \\ I_E \end{bmatrix} \tag{20}$$

$$Z_{loop} = \begin{bmatrix} Z_L+2Z_{eq} & Z_L+Z_{eq} & Z_L & 2Z_{eq} & Z_{eq} \\ Z_L+Z_{eq} & Z_L+2Z_{eq} & Z_L & Z_{eq} & 2Z_{eq} \\ Z_L & Z_L & Z_L & 0 & 0 \\ 2Z_{eq} & Z_{eq} & 0 & 2Z_{eq} & Z_{eq} \\ Z_{eq} & 2Z_{eq} & 0 & Z_{eq} & 2Z_{eq} \end{bmatrix} \quad (21)$$

Equation (18) represents five independent equations if the six diodes are conducting. However, when only two diodes are conducting, these equations are reduced to only one equation. If only three diodes are conducting these equations are reduced to only two equations, etc. [7,8]. The situation of rectifier bridge can be defined in an array named rectifier state-array S having six elements, the individual elements being 1 or 0 depending on whether the diode is conducting or not respectively [7]. The tensor [9] connecting the existing loops with those if all diodes are conducting is $C_n$. The construction of $C_n$ is obtained from the previous knowledge of S [7]. The transformation process gives the voltage and currents vector for the new networks as:

$$V_n = C_n^t E_{loop} \quad (22)$$

$$I_{loop} = C_n I_n \quad (23)$$

The new impedance matrix is given by:

$$Z_n = C_n^t Z_{loop} C_n, \quad (24)$$

from which the following equation can be written,

$$V_n = Z_n I_n \quad (25)$$

Therefore,

$$V_n = [R_n + pL_n]I_n \quad \text{and} \quad pI_n = L_n^{-1}[V_n - R_n I_n], \quad (26)$$

which may be calculated at any time t giving the current derivatives at this instant.

When all six diodes are conducting the voltage drop across each of them is zero, and equation (18)hods good. However, if any diode is open, then a voltage will appear across it. It is necessary to calculate this voltage to check whether a new diode is to be included in the conducting pattern or not. To calculate this voltage, equation (18) will be modified to the form:

$$V_x = E_{loop} - Z_{loop} I_{loop} \quad (27)$$

For the previous selected tree and cotree, we find that diode number 6 is the dependent diode; then $V_x$ is expressed as:

$$V_x = \begin{bmatrix} V_1+V_6 \\ V_2+V_6 \\ V_3+V_6 \\ -V_4+V_6 \\ -V_5+V_6 \end{bmatrix} \quad (28)$$

where $V_j$ is the voltage across the jth diode.

## EXPERIMENTAL AND SIMULATION RESULTS

For the simulation results, Euler method of numerical integration was used. The time increment for numerical integration $\Delta t$ was chosen to be 0.01 p.u. for the computer program executions. The time increment was fixed for the majority of steps, but it is varied at the switching events to give more accurate computation. For comparison purpose, results obtained from real system are compared with those obtained from digital simulation. Three tests were performed. The parameters in per unit are given in Appendix A.

Test 1: This includes switching power supply on with duty cycle equal to 0.6, and a load torque applied to the rotor shaft $T_L = 0.3838\omega_r$ p.u.

Test 2: This includes a sudden change in duty cycle from 0.0 to 1.0 after steady state has been reached (i.e. the chopper state was in the OFF mode all the time, then suddenly, the state of chopper is changed to the ON mode all the time), and a load torque applied to the rotor shaft $T_L = 0.294\omega_r$ p.u.

Test 3: This shows the steady state performance for the machine with duty cycle of the chopper equal to 0.0, and a load torque applied to the rotor shaft $T_L = 0.2203$ p.u.

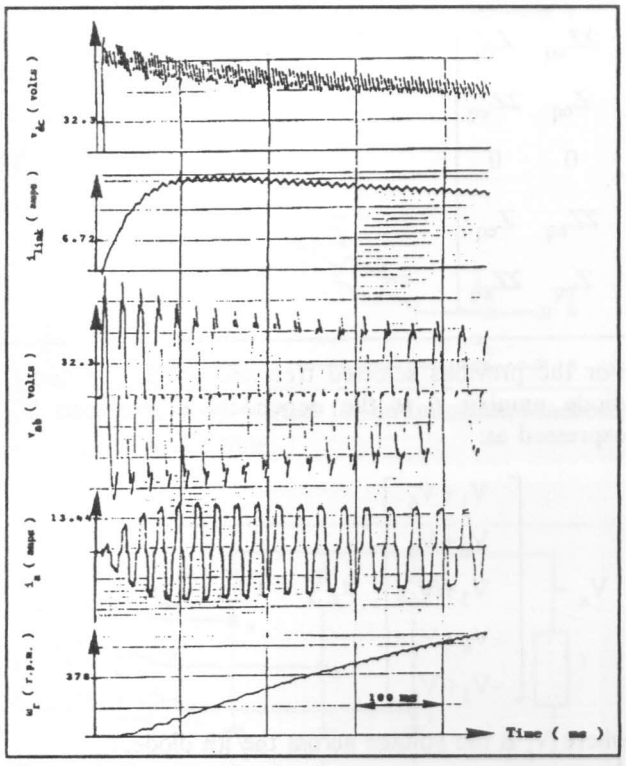


Figure 7. Test Results for Test 1.

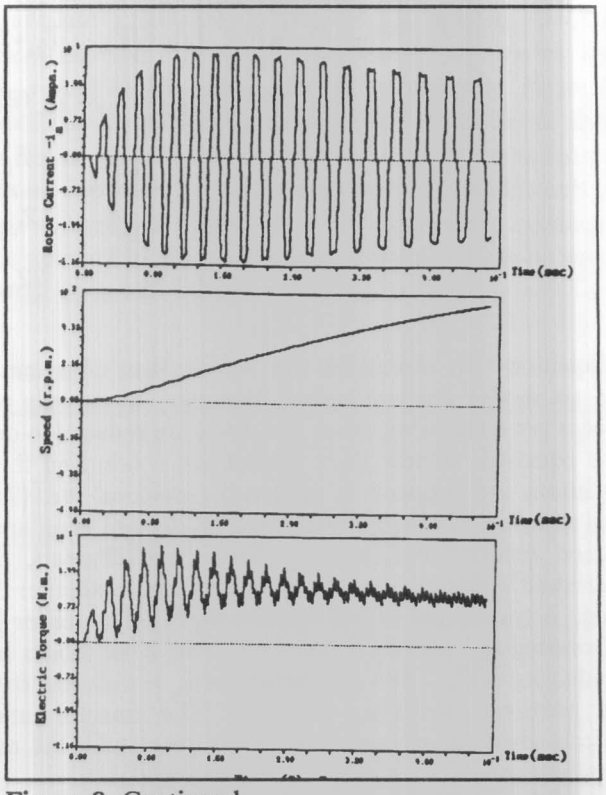


Figure 8. Continued .....

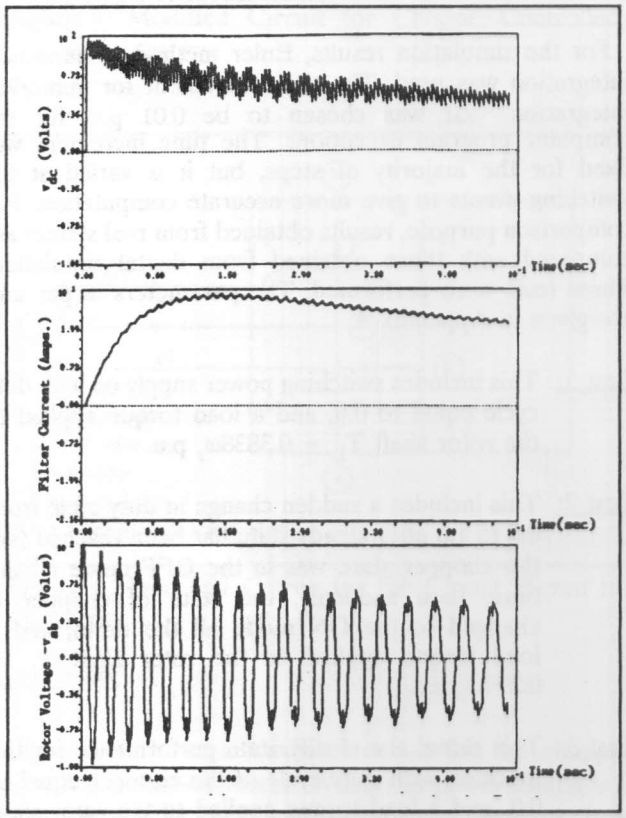


Figure 8. Digital Simulation Results for Test 1.

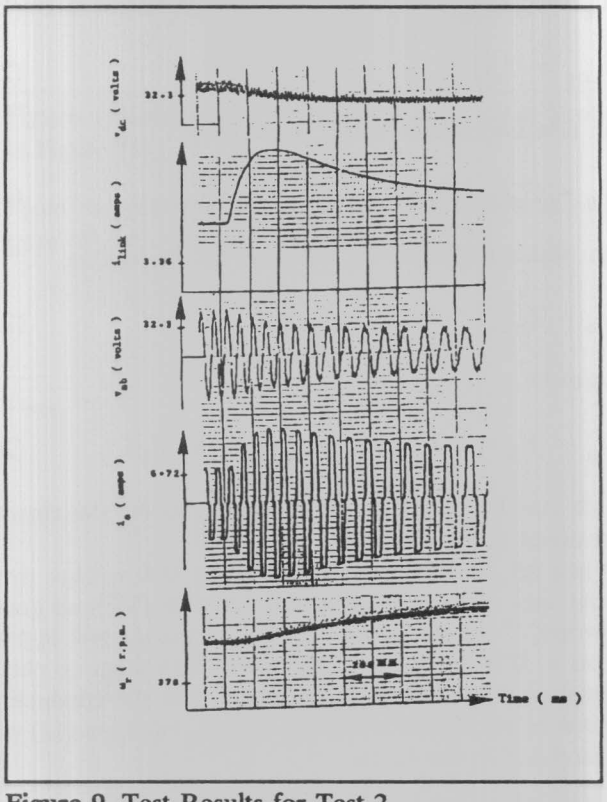


Figure 9. Test Results for Test 2.

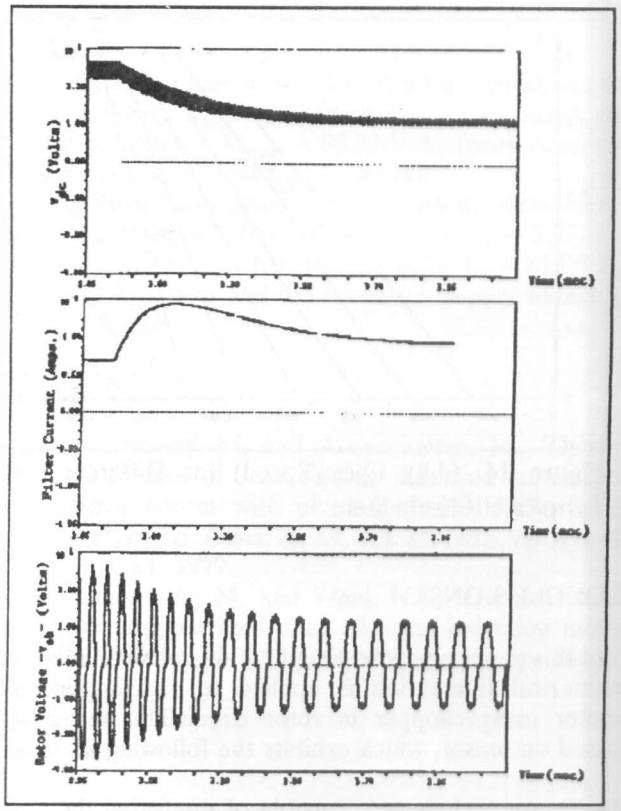


Figure 10. Digital Simulation Results for Test 2.

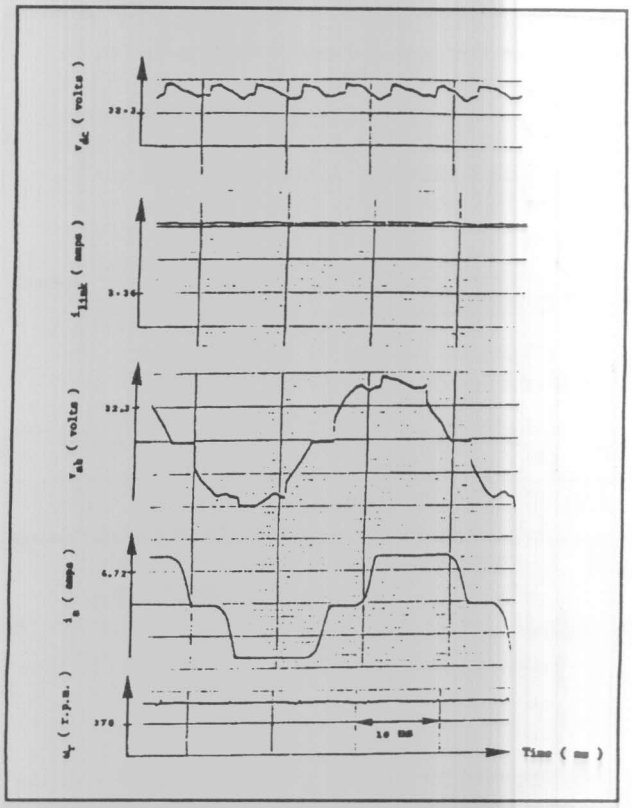


Figure 11. Test Results for Test 3.

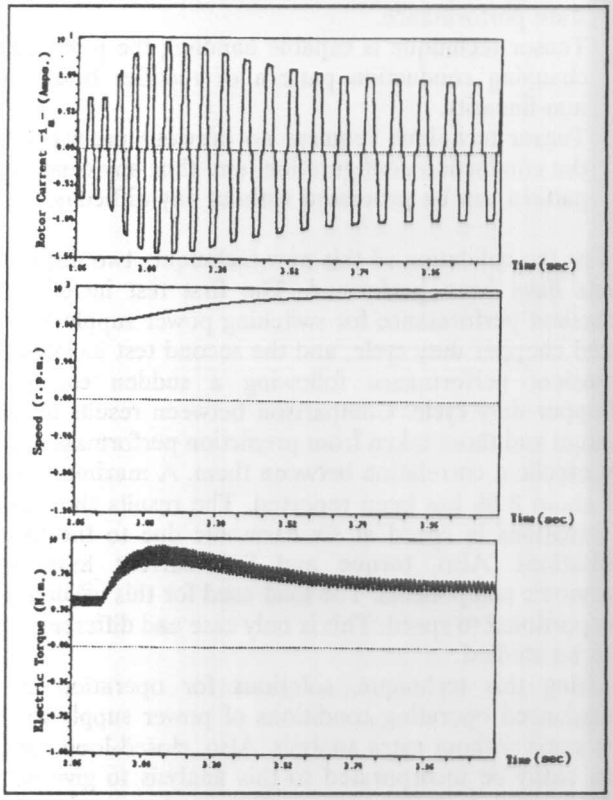


Figure 10. Continued ....

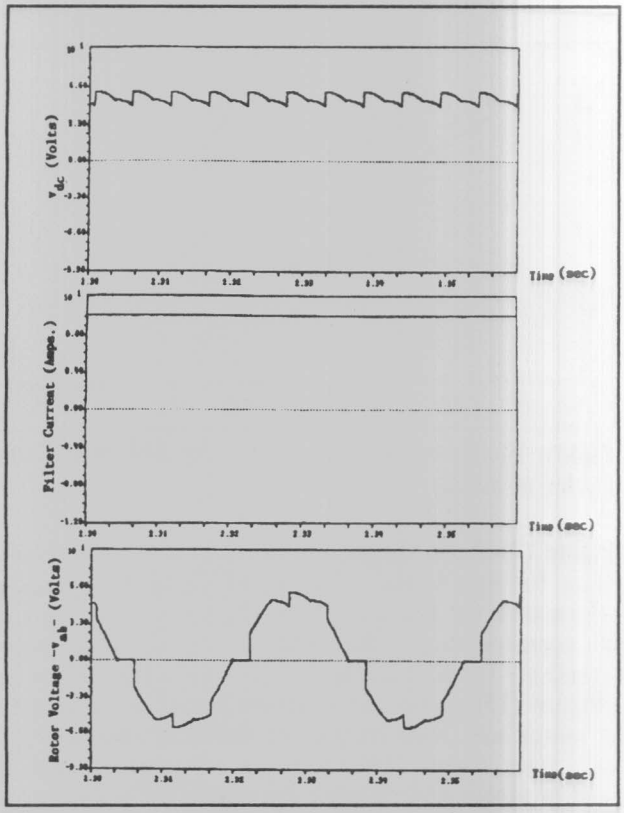


Figure 12. Digital Simulation Results for Test 3.

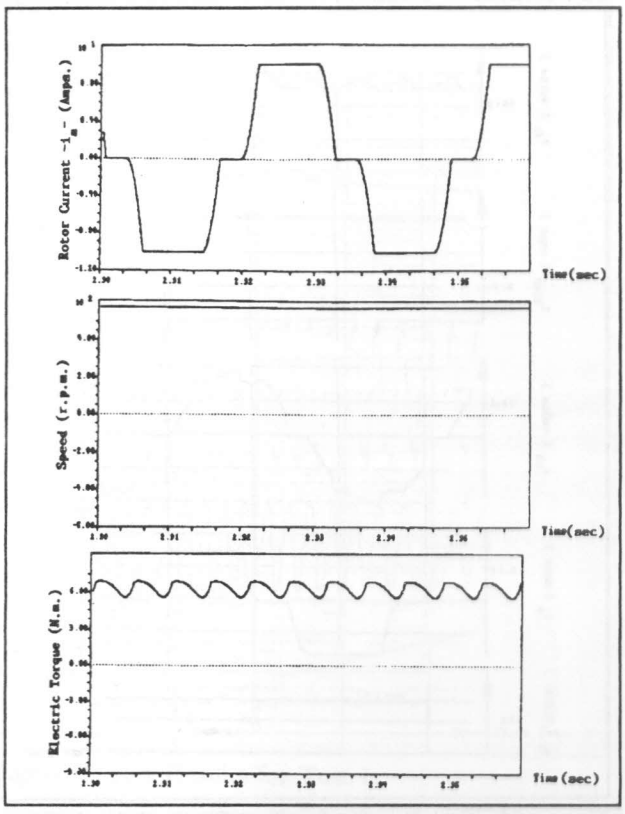


Figure 12. Continued .....

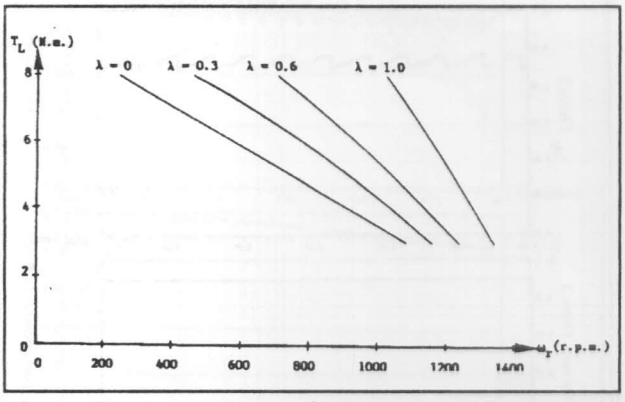


Figure 13. (Load Torque/Speed) for Different Duty Cycles at Steady State.

Figure (7) shows the system performance from the real system for test 1 while Figure (8) shows the predicted performance for the same test. Figures (9) and (10) are the corresponding real and predicted performance respectively for test 2. Figures (11) and (12) are for test 3. Figure (13) shows the relations between the speed of the motor and load torque for different duty cycles at steady state. Figure (14) shows the relations between the speed of motor and chopper duty cycle for constant load torque at steady state.

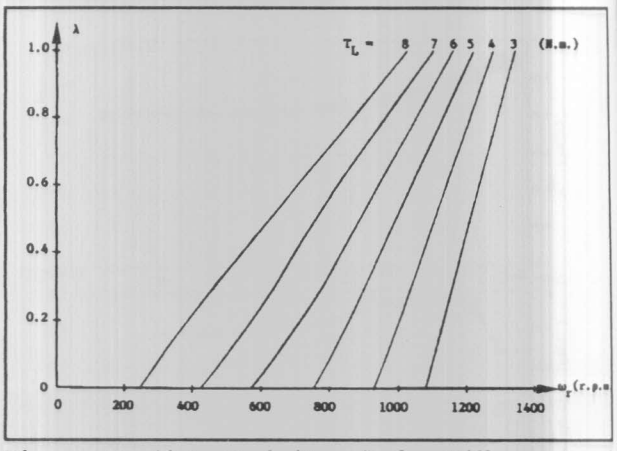


Figure 14. (duty Cycle/Speed) for Different Load Torques at Steady State.

## CONCLUSIONS

In this paper a new technique of digital simulation using numerical integration is applied to slip-ring induction motor using chopper in rotor circuit.This technique is based on tensor, which exhibits the following advantages:

1. Tensor technique is capable of predicting the various modes of operation under both transient and steady-state performance.
2. Tensor technique is capable handling the problems of changing conduction pattern of rectifier bridge and non-linearity.
3. Tensor technique requires no previous prediction for the conduction configuration, and thus any conduction pattern can be processed without any difficulty.

For the validation of this new technique, two distinctive tests have been performed. The first test includes the transient performance for switching power supply on with fixed chopper duty cycle, and the second test includes the transient performance following a sudden change in chopper duty cycle. Comparison between results for real system and those taken from prediction performance show an excellent correlation between them. A maximum error of about 8 % has been reported. The results show small fluctuations in speed at six harmonic due to the torque pulsations. Also, torque and link current have sixth harmonic components. The load used for this validation is proportional to speed. This is only case and different loads can be studied.

Using this technique, solutions for operation under unbalanced operating conditions of power supply will be the same without extra analysis. Also, closed-loop control can easily be incorporated to this analysis to give better system performance under continuous change of chopper duty cycle to achieve optimum performance.

## Appendix A

The machine used has 4 poles. The base quantities used are as follows: $I_{base}$ = 32.94 Amps. (peak rated rotor current per phase), $V_{base}$ = 89.30 Volts (peak rated rotor voltage per phase) and $f_{base}$ = 50 Hz.

Using these base quantities, the system parameters in per unit are: $R_s$ = 0.0541, $R_r$ = 0.0984, $L_s$ = 2.27, $L_r$ = 2.27, M = 2.178, J = 109, $R_F$ = 0.6724, $L_F$= 23.15, $R_{add}$ = 1.3114, $T_{CH}$ = $\pi$ and the maximum supply voltage per phase = 0.7368.

## REFERENCES


[1] Ramamoorty, M. and Arunachalam, M., "Dynamic performance of a closed loop induction motor speed control system with phase-controlled SCRs in the rotor", *IEEE Trans. on IA*, vol. 15, No.5, pp. 489-493, Sept./Oct. 1979.

[2] Ramamoorty, M. and Wani, N.S., "Dynamic model for a chopper controlled slip-ring induction motor", *IEEE Trans. on IECI*, vol. 25, No. 3, pp. 260-266, Aug. 1978.

[3] Sen, P.C. and Ma, K.H.J., "Constant torque operation of induction motors using chopper in rotor circuit", *IEEE Trans. on IA*, vol. 14, No. 5, pp. 408-414, Sept./Oct. 1978.

[4] Joshi, S.D., Dubey, G.K. and Pillai, S.K., "Extension of control range of pulse resistance controlled wound rotor induction motor", *IE(I) journal-El*, vol. 61, pp. 126-131, Dec. 1980.

[5] Hancock, N.N., *Matrix Analysis of Electrical Machinery*, Pergamon Press, Second Edition, Chapter 7, 1974.

[6] Stagg and El-Abiad, *Computer Methods in Power System Analysis*, McGraw-Hill Kogakusha, Chapter 8, 1968.

[7] Williams, S. and Smith, I.R., "Fast digital computation of 3-phase thyristor bridge circuits", *Proc. IEE*, vol. 120, No.7, pp. 791-795, July 1973.

[8] Abdelfattah, M.Y., "Converter simulation with special reference to power system disturbances", *Ph.D. Thesis*, UMIST, England, 1985.

[9] Kron, G., *Tensor analysis of network*, MacDonald, 1965.